A Spectroscopic Study of Group IV Transition Metal Incorporated Direct Templated Mesoporous Catalysts Part 1: A Comparison between Materials Synthesized Using Hydrophobic and Hydrophilic Ti Precursors

Maria E. Raimondi,[†] Enrica Gianotti,[‡] Leonardo Marchese,*[,§] Gianmario Martra,[‡] Thomas Maschmeyer,[||] John M. Seddon,[†] and Salvatore Coluccia[‡]

Department of Chemistry, Imperial College, London SW7 2AY, U.K., Dipartimento di Chimica IFM, Università di Torino, Via P. Giuria 7, I-10125 Torino, Italy, Dipartimento di Scienze e Tecnologie Avanzate, Università del Piemonte Orientale A. Avogadro, c.so Borsalino, 54, 15100 Alessandria, Italy, and Laboratory for Applied Organic Chemistry and Catalysis, TU Delft, Julianalaan 136, 2628 BL Delft, The Netherlands

Received: October 5, 1999; In Final Form: May 15, 2000

Titanium has been incorporated into mesoporous silica using novel one-pot procedures based on the true liquid crystal templating (TLCT) synthesis method. Two different Ti sources were used, one insoluble in water (titanocene dichloride) and the other completely soluble (titanium acetylacetonate). The nature of the metallic sites was investigated using diffuse reflectance UV−vis, photoluminescence and FT-IR spectroscopy. Some insight into the coordination and position of optically active species within the silica mesostructure was gained by adsorption of oxygen and ammonia probe molecules. Our results point to a particularly simple and versatile means of functionalizing mesoporous silica for catalytic applications.

Introduction

Our spectroscopic study of group IV transition metal-incorporated mesoporous silica synthesized via the true liquid crystal templating (TLCT) route is reported in two parts: Part 1 makes a comparison between two Ti-incorporated materials synthesized using different sources of titanium; part 2 will compare spectroscopic data obtained for Ti-, Zr-, and Hf-incorporated mesoporous products.[39]

The importance of titanosilicates for several catalytic applications is well established.[1] TS-1, a microporous titanium silicate containing catalytically active tetrahedral Ti(IV) sites, was first synthesized by Taramasso et al.[2] and was found to catalyze a wide range of low-temperature oxidations with hydrogen peroxide. In 1994, Corma et al. [3] published their work on framework-incorporated Ti−MCM41, and since then a considerable number of papers have been written dealing with various aspects of these materials.[4] Ti-incorporated MCM-41 can be prepared in principally two ways: (i) by grafting titanium species to the mesopore surfaces via a postsynthetic procedure[5] or (ii) by substituting Ti into the silica framework by adding a titanium alkoxide precursor to the MCM-41 synthesis gel.[3]

Previous to this work, Ti−MCM41 materials containing grafted titanium species had been studied by diffuse reflectance UV−vis, photoluminescence, and FT-IR spectroscopy.[6,7] The Ti−MCM41 (where the titanium atoms were located predominantly on the internal surfaces of the mesopores), was produced by imbibing the calcined MCM-41 structure with a chloroform solution containing bis-cyclopentadienyl titanium dichloride (titanocene dichloride).[5] When the impregnated material was exposed in situ to triethylamine (which activates the surface silanol groups of the MCM-41), the titanocene reacted with surface silanol groups, fixing itself within the mesopores. Any cyclopentadienyl ligands were then removed by calcination, leaving grafted titanium oxide sites. The material prepared in this way was found to be catalytically active in the epoxidation of cyclohexene using *tert*-butylhydroperoxide as the source of oxygen, consistent with the presence of accessible, isolated, tetrahedral Ti(IV) sites.[5]

Ti-incorporated active catalysts have also been synthesized using a one-pot process TLCT, and two different Ti sources: titaniumacetylacetonate and, as above, titanocene dichloride.[8] Here we present a spectroscopic study of these materials. TLCT of mesoporous silica was reported in 1995 by Attard et al.,[9] and the method involves the use of surfactant template in the correct aqueous concentration for the formation of a lyotropic liquid crystal phase. Hydrolysis and polymerization of the silica precursor, tetramethoxysilane (TMOS), within the aqueous regions of the liquid crystal leads to a solid silica cast surrounding the surfactant micelles. The organic portion of the as-synthesized product is then removed by calcination at 550 °C, leaving a highly regular mesoporous material. The direct relationship between the liquid crystal templating phase and the structure of the resulting solid is an advantage of the TLCT method over the Mobil MCM syntheses.[10,11] MCM syntheses use dilute surfactant templating solutions and rely on a somewhat unpredictable coprecipitation of the ordered surfactant−silicate phases, often producing significant amounts of nonstructured side products.

Experimental Section

Synthesis. A hexagonal (Type I) liquid crystal templating phase was used containing octaethylene glycol monododecyl ether, $C_{12}EO_8$ (Fluka), 10^{-2} M HCl, TMOS (Aldrich), and small amounts of titanium precursor. In the case of the metallocene-

* To whom correspondence should be addressed. E-mail: marchese@ch.unito.it.
[†] Imperial College.
[‡] Università di Torino.
[§] Università del Piemonte Orientale A. Avogadro.
[||] TU Delft.

10.1021/jp993545s CCC: $19.00
Published on Web 07/11/2000

TABLE 1: Physical Characteristic of MCM-41[10,11] and TLCT Hexagonal Mesoporous Silica (authors' data)

	calcined TLCT hexagonal mesoporous product	calcined MCM-41
d-spacing (by XRD)[a]	38 Å	40 Å
BET surface area[b]	1033 m^2/g	1000 m^2/g
pore diameter[c]	25 Å	28 Å

[a] XRD data was obtained using a small-angle Guinier line source camera. [b] B.E.T. nitrogen absorption measurements were carried out using a Micrometrics ASAP 2000 instrument. [c] Pore size was calculated using the Barret−Joyner−Hallenda (BJH) calculation.[12]

doped product, Ti[CP], the synthesis gel had the composition: 0.06 g titanocene dichloride (Aldrich)/1.5 g $C_{12}EO_8$ /1.5 mL 10^{-2} M HCl/3.165 mL tetramethoxysilane (TMOS). A 3 mL amount of methanol was used to aid dissolution of the various components in the initial synthesis gel. The framework-substituted Ti-doped material, Ti[ACAC], was synthesized using a commercial product called Tilcom TAA (Tioxide Specialities Ltd.) as the titanium source. Tilcom TAA consists of a 75 wt. % solution of di-*iso*-propoxy titanium-bis-(2,4-pentane dionate), or titanium acetylacetonate, in 2-propanol. The titanium content of Tilcom TAA is 9.9 wt. %. The Ti[ACAC] synthesis gel consisted of 20 μl Tilcom TAA/0.2 g $C_{12}EO_8$/ 200 μl 10^{-2} M HCl/422 μl TMOS. Methanol (400 Fl) was used to aid mixing of the gel components. A purely siliceous product was also made (blank) as a comparison for the metal-doped materials.

The gels were left to react overnight under light dynamic vacuum, at room temperature, to remove all of the methanol hydrolysis product. The optical textures of the products as seen by polarizing microscopy were all typical of hexagonal lyotropic phases (see results and discussion). The amount of metallocene used in the Ti[CP] synthesis was at the upper limit of solubility in the synthesis gels. In the case of Tilcom TAA, the amount used was determined by the maximum quantity accepted by the gel before losing its $C_{12}EO_8$ self-assembly properties (higher Tilcom TAA concentrations in the synthesis gels led to amorphous products).

All as-synthesized products were calcined at 500 °C heating the samples controllably at 5 °C/min under nitrogen flow, and then after 1 h at 500 °C, switching the gas flow to oxygen. After a further 8 h at 500 °C, the samples were allowed to cool to room temperature at 5 °C/min. The Ti loadings in the calcined Ti[CP] and Ti[ACAC] products were calculated from the initial synthesis compositions to be 0.92 and 1.18 wt %, respectively.

C**haracterization.** The sample was characterized by polarizing microscopy and small-angle X-ray diffraction (which also provided the *d* spacings for the ordered lattices). Mesopore diameter and BET surface area were measured by N_2 adsorption.[12] Transmission electron microscopy (TEM) provided a means to directly visualize the pore structure. Both the Ti-incorporated materials had similar structural properties and some data (measured for the blank) are presented in Table 1, together with data for MCM-41.

The calcined products were analyzed by diffuse reflectance (DR) UV−vis and UV−vis photoluminescence spectroscopy. The samples were all ground to a powder and placed in purpose-made quartz cells for spectroscopic analysis, which were attached to a vacuum-line and subjected to thermal treatments to remove all adsorbed water and organic impurities. The vacuum-line used for sample treatment reached pressures of 10^{-5} mbar by means of a diffusion pump. For oxidative treatments, a pressure of 100 Torr O_2 (0.133 bar) was used. The oxygen was introduced into the sample cell via the vacuum/Schlenk line and the quartz cell, containing the sample was heated to 550 °C using a temperature-controlled mantle.

For DR UV−vis measurements a Perkin-Elmer (Lambda 19) spectrometer equipped with an integrating sphere attachment was used. The reflectance output from the instrument was converted using the Kubelka−Munk algorithm.[13] The photoluminescence measurements were made using a Spex Fluorolog-2 (F212I) spectrometer.

For the FT-IR study, the powdered samples were compressed into thin disk-shaped pellets with a density of 2.5 mg/cm^2. The samples were mounted in a purpose-made quartz cell, which was attached to a vacuum-line similar to that used for the UV−vis in situ analyses. The samples were subjected to thermal treatments (oxidation at 550 °C) prior to the main series of measurements. The instrument used for the FTIR measurements was a Bruker IFS88 spectrometer with a resolution of 4 cm^{-1}. The final treatment for all samples before any spectroscopic measurements was an evacuation at 550 °C for 1 hour.

Catalytic Experiments. Ti[CP] and Ti[ACAC] were tested in the epoxidation of octene using *tert*-butylhydroperoxide (TBHP) as the source of oxygen.[14] Additionally Ti[CP] was also tested in the peroxidative bromination of phenol red (phenolsulfonephthalein) to tetrabromophenol blue (3′,3″,5′,5″-tetrabromophenolsufonephthalein).[15] The epoxidation reactions were carried out at 80 °C under an inert argon atmosphere, the olefin/TBHP ratio was 20 $mol \cdot mol^{-1}$ and the liquid/catalyst ratio was 75.5 $g \cdot g^{-1}$. Samples were taken from the reaction mixture at regular intervals, and the reaction products were quantified by GC analysis. Octene was in large excess and acted as the solvent as well as reactant; mesitylene was the standard for GC analysis.

Results and Discussion

Synthesis. The titanocene-doped as-synthesized material had a deep orange color, suggesting that the titanocene complex remained unhydrolyzed throughout the synthesis (hydrolysis products would have been light orange/yellow). Due to the hydrophobic nature of the cyclopentadienyl ligands, it is assumed that, at least in the as-synthesized product, the transition metal was located in the central hydrocarbon regions of the polyoxyethylene (POE) micelles (i.e., in the centers of the mesopores, see Scheme 1). The POE micelles therefore protected the complexes from the aqueous regions of the synthesis mixture, pointing to a potentially general method for mesopore functionalization.

SCHEME 1

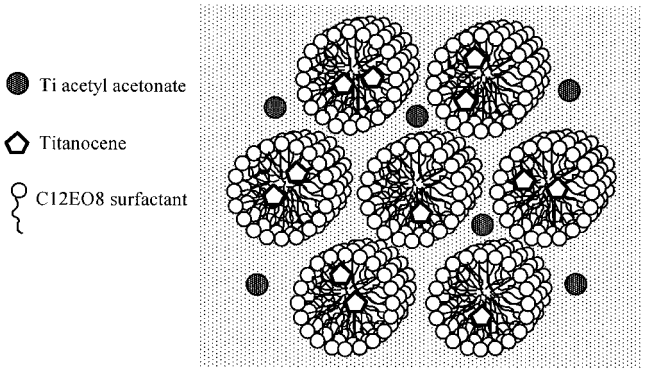

Tilcom TAA is soluble both in water and in most organic solvents. For this reason we assumed that by doping the $C_{12}EO_8$ synthesis gel, a mesoporous product would result where a large proportion of the titanium was located in the silica

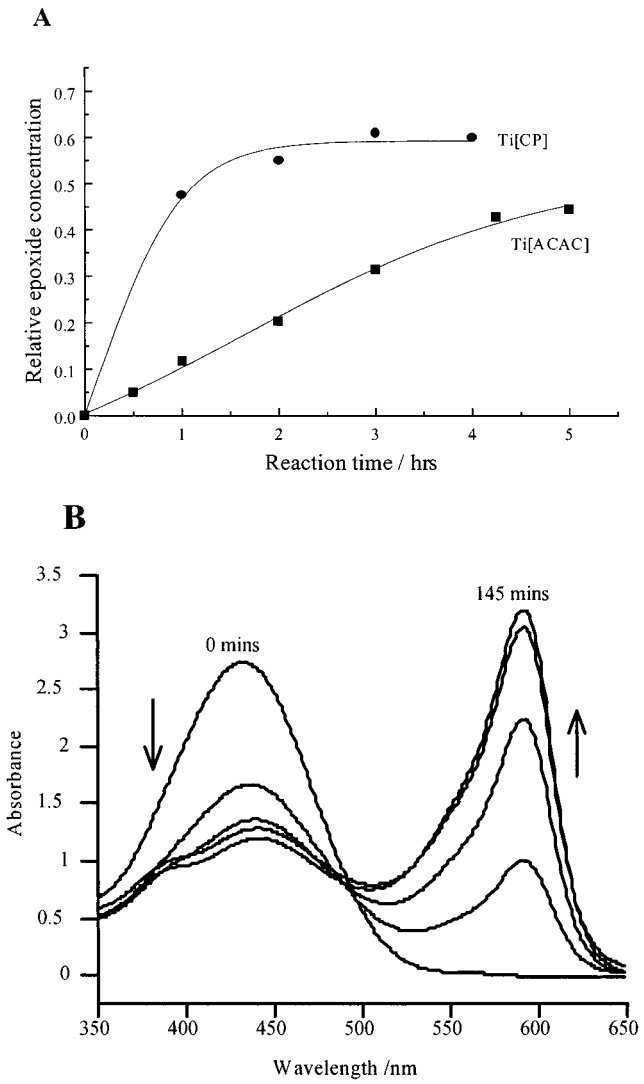

Figure 1. (A) Relative epoxide concentration formed in the oxidation of 1-octene catalyzed by Ti[CP] and Ti[ACAC]. Continuous line represents best fit to measured points. (B) UV−vis absorption spectra for peroxidative bromination test samples taken after 0, 40, 70, 110, and 145 min. Arrows indicate the effect of reaction time on band intensity.

framework rather than on the internal surfaces of the mesopores (see Scheme 1).

Catalytic Experiments. The Ti[CP] material was found to be much more active in the epoxidation of 1-octene using *tert*-butylhydroperoxide as the source of oxygen than Ti[ACAC] (Figure 1A) the conversion being 4.5 times higher after 1 h reaction. Only the Ti[CP] was tested in the peroxidative bromination of phenol red to tetrabromophenol blue, and found to be active also in this reaction (Figure 1B).

The reaction rate calculated for Ti[CP] after the first hour of reaction was 84 mol epoxide per mole Ti per hour; this value was comparable (within 30%) with the reaction rates obtained for grafted Ti−MCM41 materials[5] in a previous study. The activity of the catalysts proved that more Ti active sites are present in Ti[CP] than in Ti[ACAC].[1,4]

The peroxidative bromination test gave a qualitative indication of the catalytic activity of the catalyst, and the formation of bromophenol blue from phenol red was monitored by UV−vis spectroscopy, the Ti[CP] catalyst exhibiting slightly lower but comparable catalytic activity to the Ti−MCM materials described in the literature.[15]

Characterization. The as-synthesized TLCT materials had very similar optical textures, by polarizing microscopy, to the hexagonal lyotropic liquid crystal phase. Large transparent monolithic fragments (sometimes > 1 cm^2) of regularly structured material were formed, and calcination had little effect on the appearance of these, except for the formation of a few cracks. The optical texture under crossed polarizers after calcination was very similar to that of the as-synthesized material, shown in Figure 2A for the blank material. Powder X-ray diffraction confirmed the hexagonal symmetry of the materials, and TEM showed the presence of long, parallel channels (see Figure 2B).

Diffuse Reflectance UV−vis Spectroscopy. DR UV−vis spectroscopy allowed us to probe the nature of titanium oxide species in our titanium-doped mesoporous silica materials, and therefore assess the potential of the materials for catalytic applications. The nature of the UV absorbance of titanium-incorporated silica depends on the titanium content and on the synthesis procedure used.[16] It has been reported that for materials containing very small amounts of uniformly dispersed titanium (2.2 wt. %), it generally exists as isolated, tetrahedrally coordinated species.[7] For such materials, the electronic transition responsible for the absorption band located at $\lambda = 200-230$ nm in the DR UV−vis spectrum is a ligand metal charge transfer (LMCT) transition from oxygen to tetrahedral Ti(IV)[6,7,16−23]. [The first Laporte-allowed charge-transfer for TiX_4 complexes is related to $\pi t_1 \rightarrow de$ and $(\pi + \sigma)t_2 \rightarrow de$ or $\pi t_1 \rightarrow 3dt_2$ electron transfer[24]]. This absorption band will shift to longer wavelengths (lower energies) if the coordination of the tetrahedral Ti(IV) site is increased to values greater than 4, by bonding of molecules such as water to the reactive Ti center.

The DR UV−vis spectra for our Ti-incorporated samples reoxidized at 550 °C under static oxygen conditions are plotted in Figure 3. The spectrum for Ti[CP] had an intense maximum centered at 220 nm, which can be interpreted as evidence for the presence of titanium as isolated Ti(IV) sites within the mesoporous structure. There was also a shoulder at 250 nm and two further, much less intense bands at 330 and 460 nm, which were probably due to organic impurities resulting from the incomplete combustion of the polyoxyethylene template and/or the cyclopentadienyl ligands (see part 2 of this series of papers).[39] Ti[ACAC], recalcined at 550 °C, produced a somewhat different DR UV−vis spectrum from Ti[CP]. The band had an intensity similar to that of Ti[CP], but was displaced to 240 nm and was somewhat broadened with respect to the Ti-[CP] band. The smaller bands at higher wavelengths were not present in Ti[ACAC], suggesting that this material was free of organic impurities.

The displacement of the main adsorption peak to longer wavelength for the framework-substituted Ti[ACAC] product was likely to be due to a somewhat different chemical environment for the tetrahedrally coordinated Ti atoms in the structure. The fact that the band was broadened with respect to the Ti-[CP] material suggests that there was a greater number of chemically differing Ti sites within the Ti[ACAC] structure, absorbing at different wavelengths. The different populations of Ti−O−Si and Ti−OH species present in Ti[ACAC] and Ti[CP] would explain the differences in their absorption bands. However, the presence of TiO_2-like microclusters, which absorb at $\lambda = 250$ nm,[16] cannot be ruled out in the case of Ti[ACAC] sample.

For bulk titania (rutile or anatase phases), which is a semiconductor oxide with an easily measured optical band gap, the titanium atoms are octahedrally coordinated. For rutile titania, the absorption band in its DR UV−vis spectrum is located at 410 nm, corresponding to its band gap energy. In general, for other nonrutile titania semiconductor materials, the absorption band is located close to 350 nm.[25] Mixed TiO_2−

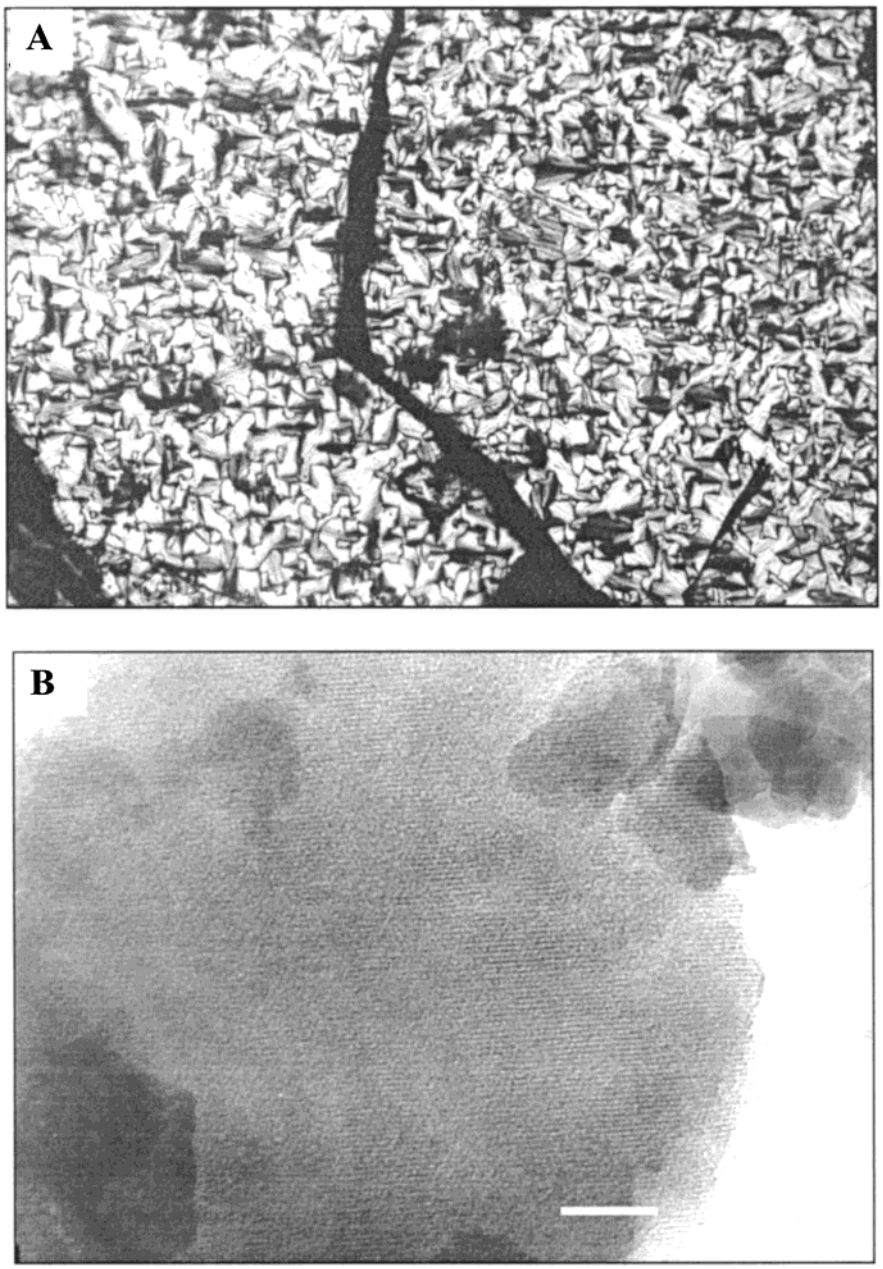

Figure 2. Calcined hexagonal TLCT mesoporous silica. (A) Polarizing micrograph (X 40; Nikon Labophot biological microscope, crossed polarizers); (B) TEM micrograph (X 150 000; 200 KV; JEOL JEM 2000 FX instrument). Scale bar: 50 nm.

SiO_2 materials provide intermediate situations between the two extremes (isolated Ti(IV) sites and pure titania) described above. The UV adsorption threshold is strongly dependent on the cluster size of the TiO_2 in the material, for cluster diameters smaller than 10 nm. This dependence on cluster size is due to the quantum size effect for semiconductors.[26] The quantum size effect can therefore be used to approximate the crystallite size of the TiO_2 clusters. UV absorption bands for such mixed oxides are located between 250 and 330 nm; for lower titania content (smaller cluster size) materials, the UV absorbance band progressively shifts to higher energies.[17] The presence of very small titania clusters in our Ti[ACAC] material is therefore possible.

For catalytic applications, isolated tetrahedral titanium oxide sites are of major interest.[1−5] Higher coordination Ti species are less effective as catalytic centers due to the lack of coordination sites for reacting molecules. For degassed Ti−MCM41 containing 2 wt. % grafted titanium, diffuse reflectance spectra contained a sharp intense absorption peak centered at 230 nm.[6,7,16] Absorption at this wavelength is an indication of the presence of tetrahedral, isolated titanium sites rather than the octahedrally coordinated titanium of titania clusters.[6,7,17]

UV−vis Photoluminescence Spectroscopy. Photoluminescence spectroscopy is another useful tool used for probing the environment and nature of titanium sites in anchored titanium oxide,[27] in Ti-framework zeolites[28] and Ti-grafted MCM-41.[6,7,16] In the case of isolated tetrahedral Ti(IV) sites, photoluminescence is due to the reverse LMCT process to that responsible for the DR UV−vis bands in the 200−230 nm range.

The photoemission spectra for materials containing tetrahedral coordinated Ti(IV) sites exhibit features in the 400 to 600 nm range,[6,7,14,28] and intense photoluminescence signals were obtained in this region for the Ti[CP] (Figure 4A) and Ti[ACAC] (Figure 4B) samples characterized by two main emission maxima at approximately 435 and 480 nm (by excitation at 250 nm). Both of these emission bands had a maximum in their excitation spectra at 240−250 nm. (Precise values of these excitation maxima could not be determined due to poor lamp intensities in the 220−240 nm range.) In agreement with the

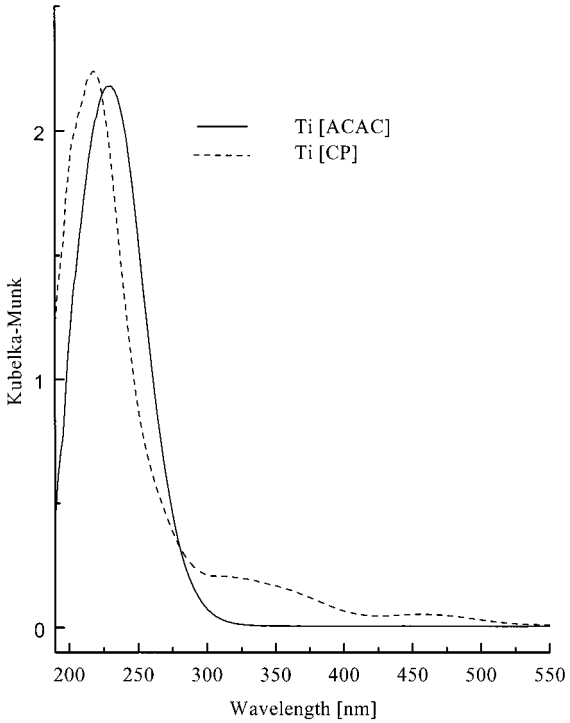

Figure 3. Diffuse reflectance UV−vis spectra for Ti[ACAC] and Ti-[CP].

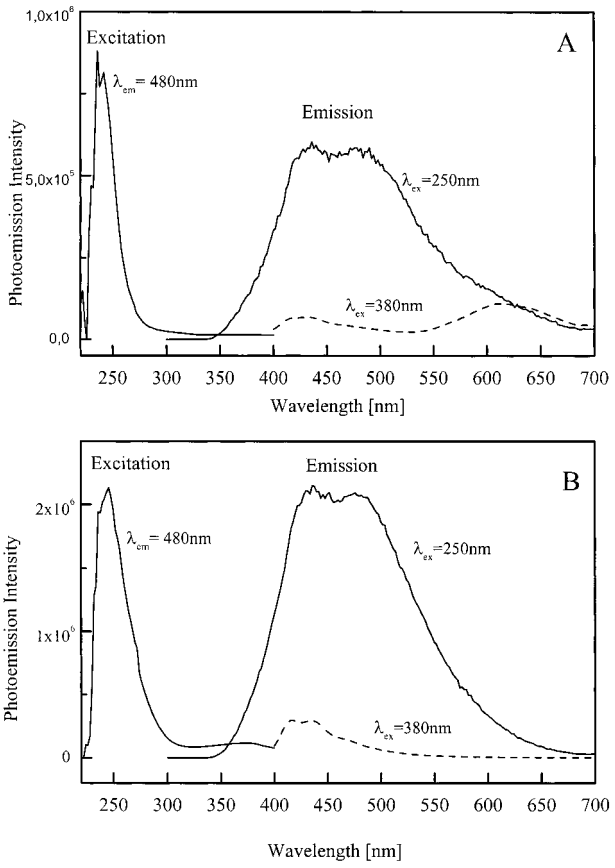

Figure 4. Photoluminescence spectra taken at 298 K, using exciting wavelengths of 250 and 380 nm (A) for Ti[CP], and (B) for Ti[ACAC]. The excitation spectra, for emission bands at 480 nm are also shown.

diffuse reflectance spectra, the excitation band for the Ti[ACAC] material was broader than for Ti[CP].

Photoluminescence spectroscopy provides a particularly useful means for probing the presence of different Ti sites in Ti-

SCHEME 2

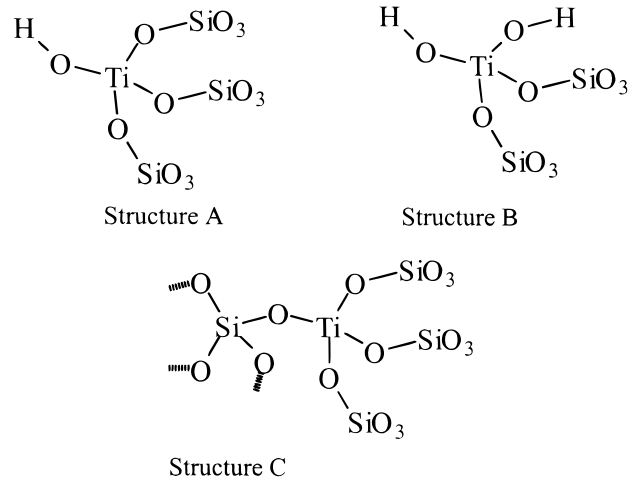

incorporated silicates. A complex emission spectrum has previously been reported for Ti−MCM41 (containing 2 wt. % grafted Ti atoms), consisting of two maxima at 434 and 480 nm and two shoulders at ca. 400 and 525−550 nm, when excited at 250 nm.[6,7] While the first two bands were assigned to two different tetrahedral Ti(IV) sites (three possible structures are represented in Scheme 2), the assignment of the other bands is still unclear.

An emission band at 495 nm for TS-1 has been recently reported and assigned to tetrahedral Ti(IV) in fully coordinated $Ti(OSi)_4$ sites[29] (structure C of Scheme 2). However, we believe that in the work conducted to date, including the results discussed in this paper, clear-cut evidence that allows the unambiguous assignment of photoemission peaks to specific tetrahedral Ti(IV) species is still lacking. In fact, we have also found that (i) dimers and/or small oligomers have a strong emission at around 500 nm,[16] and (ii) surface sites on purely siliceous mesoporous MCM-41 have a significant emission in the 500−600 nm range.[30] Research is currently being conducted, using titanium-containing silsesquioxanes as calibration samples with well-defined Ti(IV) sites, to achieve this aim. However, it is important to stress that the shapes of the photoemission spectra for the Ti-doped samples prepared using TLCT process, Ti-[CP] and Ti[ACAC], were very similar to that of carefully prepared Ti-grafted MCM-41 for which the presence of a large abundance of tetrahedral Ti(IV) sites was unequivocally established.[5,6,7]

The major difference between the photoemission spectra taken at room temperature for Ti[CP] and Ti[ACAC] was that the Ti[ACAC] emission bands were 2−3 times more intense than the Ti[CP] bands, and this might have been related to how the Ti sites were dispersed within the silica framework.[16] The intensity of the Ti[CP] band may, however, have been affected by the presence of cyclopentadiene degradation products which produced an emission peak at 610 nm when excited at 380 nm and which is not present for Ti[ACAC]. Running the spectra on Ti[CP] and Ti[ACAC] cooled to liquid nitrogen temperature (77 K) caused the emission peaks to intensify and to shift to longer wavelengths, but the relative intensity of the emission bands for Ti[CP] and Ti[ACAC] remained the same.[8]

Adsorption of oxygen onto the Ti-doped samples at room temperature only partially quenched the photoemission signals, though somewhat more for the Ti[CP] sample (Figure 5A) than for the Ti[ACAC] sample (Figure 5B). This is a significant result, as it suggests that more of the Ti(IV) sites in the Ti-[ACAC] sample were inaccessible to the oxygen than in Ti-

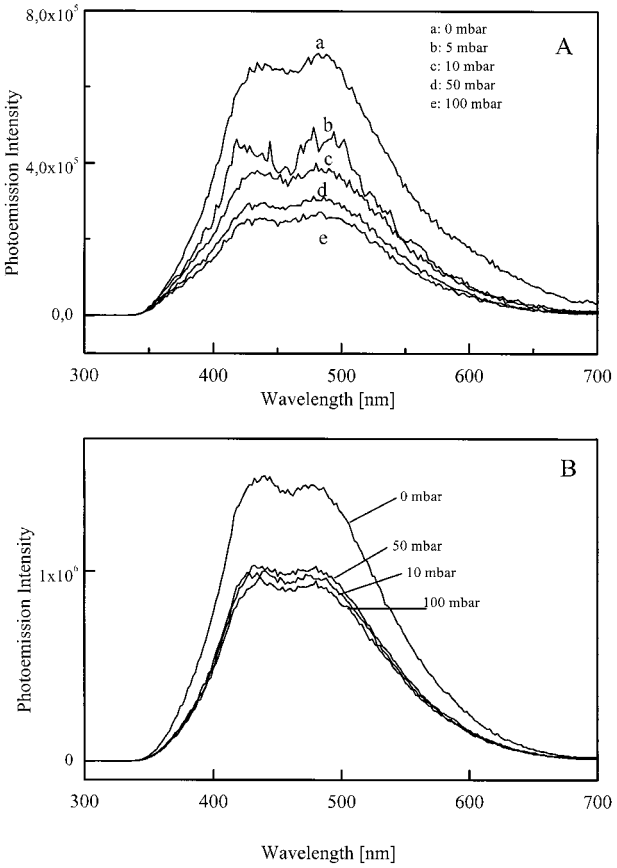

Figure 5. Effect of O_2 adsorption on the photoemission spectra of (A) Ti[CP] and (B) Ti[ACAC]. All spectra were obtained at *RT*, λ_{ex} = 250 nm.

[CP], and hence that the use of different Ti sources in the catalyst synthesis gels influences the accessibility to catalytically active sites. Even at 77 K, adsorption of 30 mbar O_2 did not cause the photoemission signal for Ti[ACAC] to lower significantly.

Fourier Transform Infra Red Spectroscopy. FT-IR was used by Marchese et al.[6,16] to characterize species present on the surface of MCM-41 and grafted Ti−MCM41. Similar studies have also been reported for TS-1[18,31,32] framework incorporated Ti−MCM41[3,33,34] and amorphous Ti-silicates.[35] NH_3 adsorption was used to monitor the acidity of surface hydroxyl groups, both in MCM-41 and grafted Ti−MCM41, and to probe the coordination of the Ti(IV) centers in the Ti−MCM41.[6]

The purely siliceous (blank) and Ti[CP] samples were studied by FTIR spectroscopy (Figure 6), and the results were compared with those obtained for grafted Ti−MCM41 reported in ref 6. We focus our attention on the Ti[CP] sample because it was found to be more active than Ti[ACAC] in the epoxidation reaction. The sharp absorption band at 3745 cm^{-1} due to the O−H stretching vibration of free hydroxyl groups was more intense for the blank sample than for the Ti[CP], suggesting that a proportion of the surface silanol groups were utilized for bonds to Ti. There was no shift in the position of this peak due to the presence of Ti in the structure.

The band at 935 cm^{-1} is evidence for the presence of Ti−O−Si bonds in Ti[CP]. It is in a very similar position to that seen for grafted Ti−MCM41 and is assigned to the antisymmetric Ti−O−Si stretching mode.[6,36]

Figure 7shows the FTIR spectra for NH_3 adsorption for both the blank and Ti[CP] samples. On the purely siliceous, blank sample (Figure 7A), NH_3 adsorbs on silanol groups and forms very weak H-bonding complexes (Scheme 3, structure A).[37] The

SCHEME 3

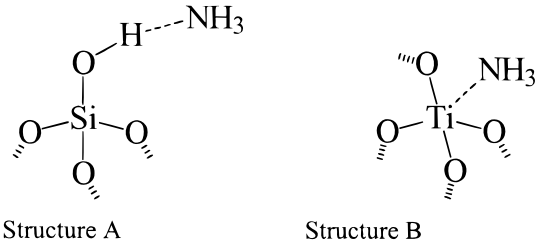

spectroscopic features of these complexes are well known, and include (i) a broad band centered at 3020 cm^{-1} due to the stretching of the H-bonded silanols, (ii) bands at 3405 and 3322 cm^{-1}, respectively, due to the NH_3 asymmetric and symmetric stretching vibrations, and (iii) a band at 1633 cm^{-1} due to the NH_3 asymmetric bending mode. The adsorption of ammonia onto the blank sample was almost completely reversible at 298 K, as demonstrated by the fact that all of the IR features associated with the complex completely disappeared, while the

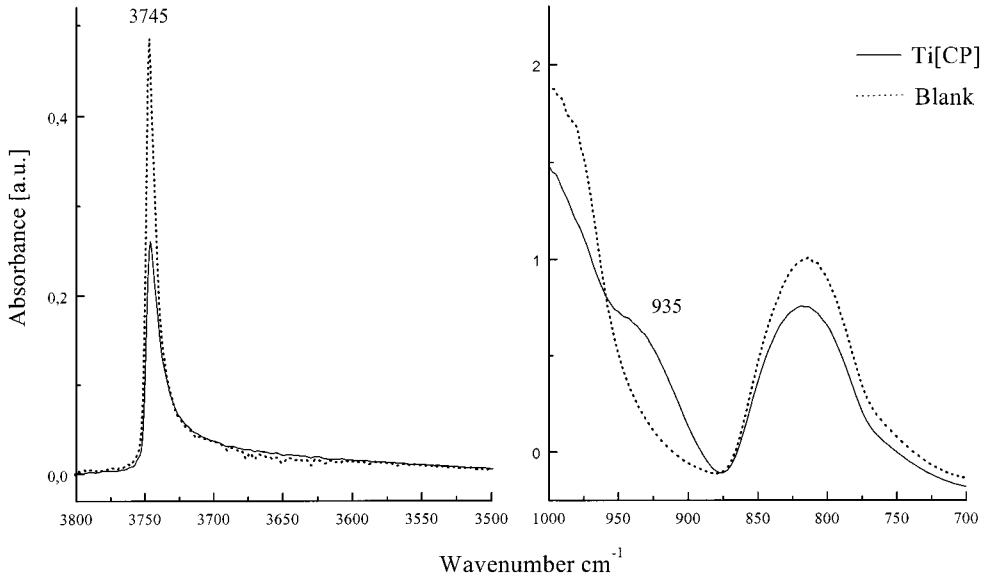

Figure 6. FTIR spectra for the blank and Ti[CP] (in vacuo).

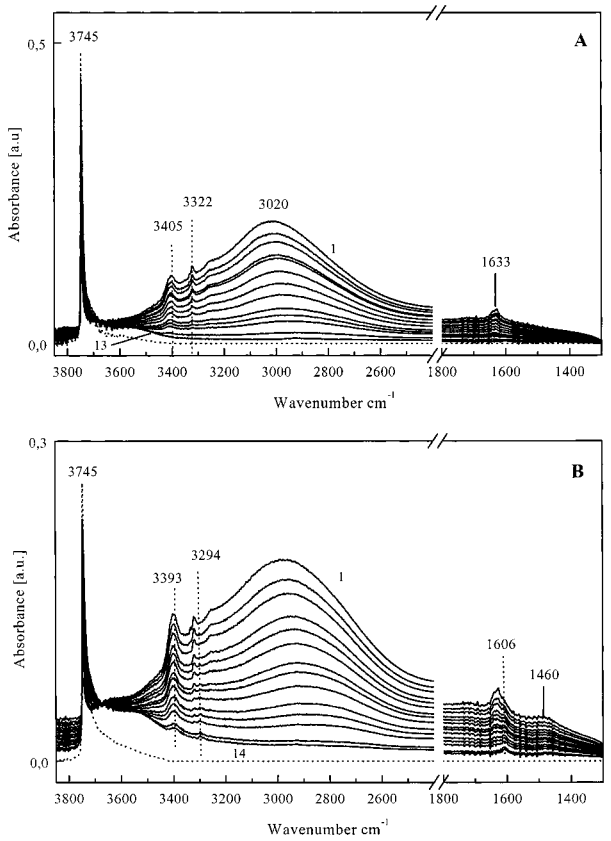

Figure 7. FTIR spectra for blank (section A) and Ti[CP] (section B) in vacuo (dotted lines) and upon NH_3 adsorption (full lines). For both materials, curve 1 corresponds to the adsorption of 30 Torr NH_3, while curves 2 to 14 correspond to decreasing doses of NH_3. Spectrum 13 (Figure 7A) was obtained by evacuating the blank sample at room temperature for 30 min, and spectrum 14 (Figure 7B) was obtained after evacuating Ti[CP] for 1 h.

narrow band at 3745 cm^{-1} was restored, upon evacuation at room temperature.

However, a broad band remained at ~3600 cm^{-1}, due to the irreversible reaction of ammonia with the most defective surface Si−O−Si bridges. This particular band was assigned to Si−OH groups formed irreversibly by reaction with ammonia;[6,38] the accompanying Si−NH_2 bending at ~1550 cm^{-1} was too weak in our case to be detected.

All of the species formed upon adsorption of ammonia on the blank were also formed on Ti[CP] (Figure 7B). However, in the latter case, further IR features at 3393, 3294, and 1606 cm^{-1}, assigned respectively to the anti-symmetric stretch, symmetric stretch, and anti-symmetric bending mode of NH_3 bonded to Ti Lewis acid sites, were observed (Scheme 3, structure B). An additional band at 1460 cm^{-1} assigned to a bending mode of NH_4^+, formed by protonation of ammonia molecules by some acidic surface hydroxyl groups, was observed only for Ti[CP]. Finally, the broad absorption in the 3400−2600 cm^{-1} range, due to the stretching vibration of H-bonded hydroxyls, was largest in the case of the Ti[CP] sample and presented a more distinct component at around 2800 cm^{-1}. This confirms that different hydroxide species were present in Ti[CP], as expected by the broadening of the 3745 cm^{-1} band.

As for Ti−MCM41,[6] the adsorption of NH_3 on Ti[CP] was not fully reversible, as indicated by the presence of weak bands at 3393, 3294, 1606, and 1460 cm^{-1} associated with Ti−NH_3 complexes after evacuation of the Ti[CP] sample for 1 h at room temperature. A broad shoulder at 3550 nm also remained after removing the ammonia from the Ti[CP] sample. The species responsible for this shoulder are difficult to assign precisely, but are likely to be H-bonded hydroxyl groups formed irreversibly as a result of ammonia adsorption.

Conclusions

It has been demonstrated that the TLCT synthesis route can be used to incorporate Ti catalytic sites into the silica mesoporous products in a controllable way. The nature of the transition metal precursor, hydrophobic or hydrophilic, determines whether the catalytic species will be accessible, within the mesopores or buried in the silica walls.

UV−vis and IR spectroscopic analyses of TLCT mesoporous silica doped with titanium have provided some very interesting data, shedding light on the nature of the transition metal sites and on their accessibility for probe molecules. In the case of Ti[CP], our spectroscopic data confirm that the Ti existed mainly as isolated tetrahedral Ti(IV) oxide, with very few, if any, Ti−O−Ti bonds. The Ti centers were accessible to gaseous molecules as proven by UV−vis photoluminescence signal quenching when O_2 was adsorbed into the structure, and NH_3 adsorption in the FTIR measurements. The potential for these materials in catalytic applications is therefore established.

In Part 2 the use of metallocene precursors for the incorporation of zirconium and hafnium into mesoporous silica is described,[39] and spectroscopic data for the products are compared with those obtained for the Ti[CP] analogue.

Acknowledgment. M.E.R thanks the British EPSRC for a studentship. Financial support from the Italian CRUI (Conferenza dei Rettori delle Università Italiane) and MURST (Ministero della Ricerca Scientifica e Tecnologica) is also gratefully acknowledged. We further acknowledge the experimental contribution of Dr. Ziping Shan (TUD).

References and Notes

(1) Notari, B. *Adv. Catal.* **1996**, *41*, 252.
(2) Taramasso, M.; Perego, G.; Notari, B. U.S. Patent 4,410,501 (1983).
(3) Corma, A.; Navarro, M. T.; Pariente, J. P. *Chem. Commun.* **1994**, 147.
(4) (a) Maschmeyer, T. *Curr. Op. Solid State Mater. Sci.* **1998**, *3*, 71. (b) Thomas, J. M. *Philos. Trans. R. Soc.* **1990**, *A333*, 173. See also *Nature* **1994**, *368*, 289. (c) Tanev, P. T.; Chibwe, M.; Pinnavaia, T. J. *Nature* **1994**, *368*, 321. (d) Zhang, W.; Fröba, M.; Wang, J.; Tanev, P. T.; Wong, J.; Pinnavaia, T. J. *J. Am. Chem. Soc.* **1996**, *118*, 9164.
(5) Maschmeyer, T.; Rey, F.; Sankar, G.; Thomas, J. M. *Nature* **1995**, *378*, 159.
(6) Marchese, L.; Gianotti, E.; Maschmeyer, T.; Martra, G.; Coluccia, S.; Thomas, J. M. *Il Nuovo Cimento* **1997**, *19*, 1707.
(7) Marchese, L.; Maschmeyer, T.; Gianotti, E.; Coluccia, S.; Thomas, J. M. *J. Phys. Chem. B* **1997**, *101*, 8836.
(8) Raimondi, M.; Marchese, L.; Gianotti, E.; Maschmeyer, T.; Seddon, J. M.; Coluccia, S. *Chem. Commun.* **1999**, 87.
(9) Attard, G. S.; Glyde, J. C.; Göltner, C. G. *Nature* **1995**, *378*, 366.
(10) Beck, J. S.; Vartuli, J. C.; Roth, W. J.; Leonowicz, M. E.; Kresge, C. T.; Schmitt, K. D.; Chu, C. T. W.; Olson, D. H.; Sheppard, E. W.; McCullen, S. B.; Higgins, J. B.; Schlenker, J. L. *J. Am. Chem. Soc.* **1992**, *114*, 10834.
(11) Kresge, C. T.; Leonowicz, M. E.; Roth, W. J.; Vartuli, J. C.; Beck, J. S. *Nature* **1992**, *359*, 710.
(12) (a) Gregg, S. J.; Sing, K. S. W. *Surface Area and Porosity*, 2nd edition; Academic Press: San Diego, 1995. (b) Barret, E. P.; Joyner, L. G.; Halenda, P. P. *J. Am. Chem. Soc.* **1951**, *73*, 373.
(13) Kortüm, G. *Reflectance Spectroscopy*; Springer-Verlag: Berlin, 1969.
(14) Crocker, M.; Herold, R. H. M.; Orpen, A. G. *Chem. Commun.* **1997**, 2411.
(15) Walker, J. V.; Morey, M.; Carlsson, H.; Davidson, A.; Stucky, G. D.; Butler, A. *J. Am. Chem. Soc.* **1997**, 119, 6921.
(16) Marchese, L.; Maschmeyer, T.; Gianotti, E.; Dellarocca, V.; Rey, F.; Coluccia, S.; Thomas, J. M. *Phys. Chem. Chem. Phys.* **1999**, *1*, 585.
(17) Davis, R. J.; Liu, Z. F. *Chem. Mater.* **1997**, *9*, 2311.
(18) Boccuti, M. R.; Rao, K. M.; Zecchina, A.; Leofanti, G.; Petrini, G. *Stud. Surf. Sci. Catal.* **1989**, *48*, 133.

(19) Geobaldo, F.; Bordiga, S.; Zecchina, A.; Giamello, E.; Leofanti, G.; Petrini, G. *Catal. Lett.* **1992**, *16*, 109.
(20) Bordiga, S.; Coluccia, S.; Lamberti, C.; Marchese, L.; Zecchina, A.; Boscherini, F.; Buffa, F.; Genoni, F.; Leofanti, G.; Petrini, G.; Vlaic, G *J. Phys. Chem.* **1994**, *98*, 4125.
(21) Klaas, J.; Schulz-Ekloff, G.; Jaeger, N. I. *J. Phys. Chem. B* **1997**, *101*, 1305.
(22) Klein, S.; Weckhuysen, B. M.; Martens, J. A.; Maier, W. F.; Jacobs, P. A. *J. Catal.* **1996**, *163*, 489.
(23) Lenoc, L.; On, D. T.; Solomykina, S.; Echchahed, B.; Beland, F.; Moulin, C. C. D.; Bonneviot, L. *Stud. Surf. Sci. Catal.* **1996**, *101*, 611.
(24) Jørgensen, C. K. *Prog. Inorg. Chem.* **1970**, *12*, 101.
(25) Grant, F. A. *Rev. Modern Phys.* **1959**, *31*, 646.
(26) Lange, F. F.; Miller, K. T. *Adv. Ceram. Mater.* **1987**, *2*, 827.
(27) (a) Yamashita, H.; Ichihashi, Y.; Anpo, M.; Hashimoto, M.; Louis, C.; Che, M. *J. Phys. Chem.* **1996**, *100*, 16041. (b) Anpo, M.; Aikawa, N.; Kubokawa, Y.; Che, M.; Louis, C.; Giamello, E. *J. Phys. Chem.* **1985**, *89*, 5017.
(28) (a) Zhang, S. G.; Ichihashi, Y.; Yamashita, H.; Tatsumi, T.; Anpo, M. *Chem. Lett.* **1996**, 895. (b) Ichihashi, Y.; Yamashita, H.; Anpo, M.; Souma, Y.; Matsumura, Y. *Catal. Lett.* **1998**, *53*, 107.
(29) Lamberti, C.; Bordiga, S.; Arduino, D.; Zecchina, A.; Geobaldo, F.; Spanò, G.; Genoni, F.; Petrini, G.; Carati, A.; Villain, F.; Vlaic, G. *J. Phys. Chem. B* **1998**, *102*, 6382.
(30) Yoshida, H.; Marchese, L. *Phys. Chem. Lett.*, submitted.
(31) Scarano, D.; Zecchina, A.; Bordiga, S.; Geobaldo, F.; Spoto, G.; Petrini, G.; Leofanti, G.; Padovan, M.; Tozzola, G. *J. Chem. Soc., Faraday Trans.* **1993**, *89*, 4123.
(32) Astorino, E.; Peri, J. B.; Willey, R. J.; Busca, G. *J. Catal.* **1995**, 157, 482.
(33) Blasco, T.; Corma, A.; Navarro, M. T.; Pariente, J. P. *J. Catal.* **1995**, *156*, 65.
(34) Alba, M. D.; Luan, Z. H.; Klinowski, J. *J. Phys. Chem.* **1996**, *100*, 2178.
(35) Klein, S.; Thorimbert, S.; Maier, W. F. *J. Catal.* **1993**, *163*, 476.
(36) de Man, A. J. M.; Sauer, J. *J. Phys. Chem.* **1996**, *100*, 5025.
(37) Sauer, J.; Ugliengo, P.; Garrone, E.; Saunders: V. R. *Chem. Rev.* **1994**, *94*, 2095.
(38) Morrow, B. A.; Cody, I. A. *J. Phys. Chem.* **1976**, *80*, 1998.
(39) Gianotti, E.; Raimondi, M. E.; Marchese, L.; Martra, G.; Maschmeyer, T.; Seddon, J. M.; Coluccia, S. *Phys. Chem. Chem. Phys.*, submitted.